Development 127, 1039-1048 (2000)
Printed in Great Britain © The Company of Biologists Limited 2000
DEV9680

Functional conservation of *atonal* and *Math1* in the CNS and PNS

Nissim Ben-Arie[2,3,*], Bassem A. Hassan[1,2], Nessan A. Bermingham[1,3], Denise M. Malicki[4], Dawna Armstrong[4], Martin Matzuk[2,4,5,6], Hugo J. Bellen[1,2,6] and Huda Y. Zoghbi[1,2,3,6,‡]

[1]Howard Hughes Medical Institute and Departments of [2]Molecular and Human Genetics, [3]Pediatrics, [4]Pathology, [5]Cell Biology and [6]Program in Developmental Biology, Baylor College of Medicine, One Baylor Plaza, Houston, Texas 77030, USA

*Present address: Cell and Animal Biology, The Hebrew University of Jerusalem, Givat-Ram, Jerusalem 91904, Israel

‡Author to whom correspondence should be addressed (e-mail: hzoghbi@bcm.tmc.edu)

Accepted 9 December 1999; published on WWW 8 February 2000

SUMMARY

To determine the extent to which *atonal* and its mouse homolog *Math1* exhibit functional conservation, we inserted β-galactosidase (*lacZ*) into the *Math1* locus and analyzed its expression, evaluated consequences of loss of *Math1* function, and expressed *Math1* in *atonal* mutant flies. *lacZ* under the control of *Math1* regulatory elements duplicated the previously known expression pattern of *Math1* in the CNS (i.e., the neural tube, dorsal spinal cord, brainstem, and cerebellar external granule neurons) but also revealed new sites of expression: PNS mechanoreceptors (inner ear hair cells and Merkel cells) and articular chondrocytes. Expressing *Math1* induced ectopic chordotonal organs (CHOs) in wild-type flies and partially rescued CHO loss in *atonal* mutant embryos. These data demonstrate that both the mouse and fly homologs encode lineage identity information and, more interestingly, that some of the cells dependent on this information serve similar mechanoreceptor functions.

Key words: *atonal*, *Math1*, CNS, PNS, *Drosophila melanogaster*, Mouse, Mechanoreceptors

INTRODUCTION

During evolution primitive cellular machinery is constantly being co-opted for new purposes. An example of this strategy is the development of balance and audition organs. In *Drosophila*, *atonal* (*ato*) controls the development and function of chordotonal organs (CHOs), the sensory elements which provide proprioception and vibration sense (Eberl, 1999; McIver, 1985; van Staaden and Römer, 1998). CHOs populate the peripheral nervous system (PNS) in the body wall and joints (thorax, abdomen, sternum, wings, legs) and antennae (Moulins, 1976), providing the fly with sensory information much as touch and mechanoreceptors do in vertebrates (McIver, 1985; Moulins, 1976). Boyan (1993) proposed that, in the course of evolution, different CHOs became specialized for hearing in different insects. This hypothesis was recently confirmed by van Staaden and Römer (1998). In *Drosophila*, CHOs in the Johnston organ, located in the second antennal segment, function in near field hearing (Dreller and Kirschner, 1993; Eberl, 1999) and negative geotaxis (B. H. and H. J. B., unpublished data).

During development *ato* is expressed in a cluster of progenitor cells from which the CHO founder cells are selected (Jarman et al., 1993). It likely functions by regulating the expression of genes necessary for the specification and development of the CHO lineage, as it encodes a basic helix-loop-helix protein (bHLH) that dimerizes with the Daughterless protein and binds to E-box sequences (Jarman et al., 1993). CHO specificity is encoded by the *ato* basic domain, which is required for DNA binding in bHLH proteins (Chien et al., 1996; Davis et al., 1990; Jarman and Ahmed, 1998; Vaessin et al., 1990). *ato* is both necessary and sufficient for the generation of CHOs in the fly: loss of *ato* function leads to the loss of CHOs, while ectopic *ato* expression causes ectopic CHO formation (Jarman et al., 1993).

Because of *ato*'s importance in *Drosophila* peripheral nervous system (PNS) development**,** a number of laboratories have searched for *ato* homologs in various species. Interestingly, the mouse homologs (*Math4A*/neurogenin2, *Math4C*/neurogenin1, *Math3* and *Math5*) are expressed not just in the PNS, but in the central nervous system (CNS) at various developmental stages and in different anatomical structures (Fode et al., 1998; Ma et al., 1998; Takebayashi et al., 1997).

Mouse atonal homolog 1 (*Math1)* is one of *ato*'s closest known homologs, with 82% amino acid similarity in the bHLH domain and 100% conservation of the basic domain that determines target recognition specificity (Ben-Arie et al., 1996; Chien et al., 1996). *Math1* is transiently expressed in the CNS starting at embryonic day 9 (E9) in the dorsal portion of the neural tube. *Math1* is also expressed in the rhombic lip of the fourth ventricle of the brain, where cerebellar granule cell precursors are born at E13-15 (Alder et al., 1996). Upon proliferation and differentiation, these progenitor cells migrate to form the external granule layer (EGL) of the cerebellar primordia (Hatten and Heintz, 1995). Proliferating EGL cells continue to express *Math1* during the first three postnatal weeks, until shortly before they migrate to their final adult destination to generate the internal granule layer (IGL) of the cerebellum (Akazawa et al., 1995; Ben-Arie et al., 1996). Another group of cells, a small population of neuronal precursors in the dorsal spinal cord, expresses *Math1* during E10-E14 (Akazawa et al., 1995; Ben-Arie et al., 1996). These precursor cells also express the LIM homeodomain proteins (LH2A and LH2B), markers of the D1 class of commissural interneurons (Lee et al., 1998). Helms and Johnson (1998) reported that *lacZ* expression under the control of *Math1* regulatory elements reproduced *Math1* expression patterns in the developing cerebellum and spinal cord, and demonstrated that *Math1* is expressed in precursors that give rise to a subpopulation of dorsal commissural interneurons.

To determine the in vivo function of *Math1*, we previously generated mice ($Math1^{m1/m1}$) lacking the MATH1 protein. This null mutation causes major cerebellar abnormalities: lack of granule cell proliferation and migration from the rhombic lip at E14.5, and absence of the entire EGL at birth (Ben-Arie et al., 1997). It is not clear whether the agenesis of cerebellar granule neurons is due to failure of progenitor specification or the cells' inability to proliferate and/or differentiate. Neonates cannot breathe and die shortly after birth, but there are no gross defects in any cranial nerves or brain stem nuclei that could explain respiratory failure.

Although *ato* and *Math1* share a high degree of sequence conservation, there is an apparent discrepancy between their expression patterns and the consequences of their loss of function. Whereas *ato* is expressed primarily in the PNS of the fly and its absence causes loss of almost all CHOs (Jarman et al., 1993), *Math1* is expressed in the CNS and its loss leads to absence of cerebellar granule neurons, the largest neuronal population in the CNS (Ben-Arie et al., 1997). To better understand the functional relations between *ato* and *Math1*, we generated a second *Math1* null allele in mice ($Math^{\beta\text{-}gal/\beta\text{-}gal}$) by replacing the *Math1* coding region with a β-galactosidase gene (*lacZ*) and searched for CNS expression of *ato* in the fruit fly. Our results confirm the functional link between *ato* and *Math1*: *ato* is expressed in the fly brain, and *lacZ* expression under the control of *Math1* regulatory elements (*Math1/lacZ*) not only replicated the known expression pattern in the CNS (i.e., the neural tube, spinal cord and cerebellum), but appeared in many other cells of the murine PNS. Overexpression of *Math1* in *Drosophila* caused ectopic CHO formation, providing further insight into the relationship between the two genes.

MATERIALS AND METHODS

Generation of *Math1* knock-in mice

To delete the entire coding region of *Math1*, we generated a targeting construct that contained the 5′ and 3′ genomic flanking fragments as described previously (Ben-Arie et al., 1997) flanking a pSAβgal/PGK-neo cassette (Friedrich and Soriano, 1991). The construct is designed so that *lacZ* expression is driven by endogenous *Math1* control elements, while an independent PGK promoter drives the expression of the selectable marker *neo*.

The construct was electroporated into ES cells and selection for *neo* was achieved with G418. Fourteen out of 76 (18%) clones underwent homologous recombination. Genotyping of ES cells, yolk sac and tail DNA was performed using Southern analysis of *Eco*RI digested DNA and probes previously described (Ben-Arie et al., 1997).

X-gal staining, histological and immunohistochemical analyses

Embryos were staged by designating the morning of the vaginal plug as E0.5. Embryos were dissected out of the uterus, separated from extraembryonic membranes, and placed in cold phosphate-buffered saline (PBS). The embryos were then fixed in 4% paraformaldehyde (PFA) in PBS for 30 minutes, and washed in cold PBS. Yolk sacs or tails were collected before fixation for DNA extraction and genotyping. Equilibration to improve the penetrability of the staining reagents was performed in 0.02% NP40, 0.01% sodium deoxycholate in PBS for 10 minutes at room temperature. Whole-mount staining with X-gal (Bonnerot and Nicolas, 1993) was performed for 16-24 hours at 30°C while shaking in the same equilibration buffer, which also contained 5 mM potassium ferricyanide, 5 mM potassium ferrocyanide, and 40 mg/ml X-gal (dissolved in DMSO). When the desired intensity of staining was achieved, usually within 18 hours, embryos were washed in PBS, postfixed for 30 minutes in buffered formalin, serially dehydrated in 25, 50 and 70% ethanol, and stored at 4°C.

For histological analysis embryos were further dehydrated in 80, 90 and 100% ethanol, treated in Histoclear (National Diagnostics), and embedded in Paraplast (Oxford Labware). 7-20 μm sections were cut using in a microtome (Microme). Counterstaining was performed using nuclear fast red (Vector Laboratories). Immunohistochemistry was performed as detailed previously (Ben-Arie et al., 1997). Antibodies: anti-cytokeratin 18 (DAKO) 1:20; anti-human chromogranin A (DAKO) 1:100; anti-MATH1 (see below) 1:200.

Generation of anti-MATH1 antibody

An *Eco*RI-*Hin*dIII fragment encoding the N-terminal 156 amino acids of the MATH1 open reading frame (*Math1*Δ) was cloned into the pET 28a+ expression vector (Novagen). *Math1*Δ fragment was expressed as a His tag fusion protein. Soluble MATH1Δ protein was purified according to His-tag kit specifications (Novagen) and 2 mg of protein were used to immunize Chickens (Cocalico Biologicals Inc.).

Analysis of Tabby mice

Ta/Ta females were kindly provided by Dr P. Overbeek (Baylor College of Medicine, Houston, TX). These were time-mated with $Math1^{+/\beta\text{-}gal}$ males, and embryos were harvested at E16.5. Each pup's gender was determined by PCR on tail DNA, using primers (forward TGAAGCTTTTGGCTTTGAG, and reverse CCGCTGCCAAA-TTCTTTGG) that yielded a 320 bp product from chromosome X, and a 300 bp product from chromosome Y (Liu et al., 1999). Amplification conditions were: 92°C/1 minute, 55°C/1 minute, 72°C/1 minute for 32 cycles, with an initial denaturation step of 94°C/7 minutes and last extension step of 72°C/7 minutes. Amplification products were separated on 2% agarose gels. X-gal-stained embryos were scored independently by 2 individuals, and only then were results matched with the determined gender.

Ectopic expression of *Math1* in flies

yw flies were transformed with a *UAS-Math1* construct as described by Brand and Perrimon (1993). To overexpress *Math1* in wild-type flies, *yw*; *UAS-Math1* flies were mated to *HS-Gal4* flies. The progeny were heat shocked as described previously (Jarman et al., 1993). To rescue the loss of chordotonal organs in *ato* mutant flies, *w*; *UAS-Math1*/*UAS-Math1*; *ato1/TM6* flies were crossed to *w*; *HS-Gal4/CyO*; *ato1/TM6* flies. Embryos were collected for 3 hours, aged for 3 hours, heat shocked for 30 minutes at 37°C and allowed to develop for the next 12-15 hours. Embryos were fixed in 4% formaldehyde in PBS with 50% heptane. Embryos were washed with 100% ethanol, transferred to PBT and stained with mAb 22C10 as described previously (Kania et al., 1995) to detect PNS neurons. Chordotonal neurons were identified by their distinct morphology and position.

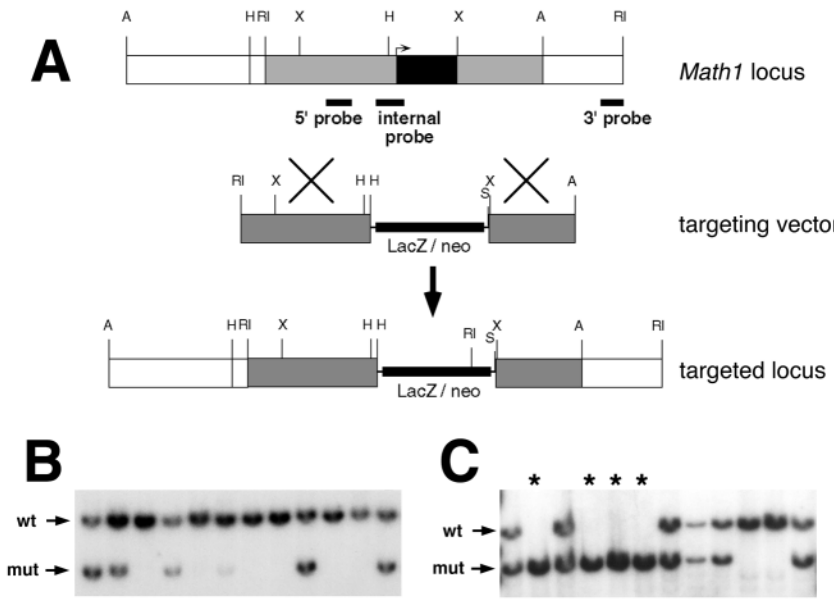

Fig. 1. Replacement of *Math1* coding region by the *lacZ* gene. (A) Top, map of the *Math1* genomic locus. The coding region is shown as a black box. The sites of the probes used to detect the wild-type and mutant alleles are shown as black bars. The targeting vector is in the middle with the sites for homologous recombination indicated by large Xs. In the targeted locus shown at the bottom, *lacZ* is translated under the control of *Math1* regulatory elements. (B) Southern blot analysis of embryonic stem cells using the 3′ external probe. The upper band represents the wild-type allele and the lower band the targeted mutant allele (mut) in targeted clones. (C) Southern blot analysis of DNA from the progeny of heterozygous mice demonstrating the presence of the targeted allele and absence of the wild-type allele in *Math1*$^{\beta\text{-}gal/\beta\text{-}gal}$ mice (asterisks). A, *Apa*I; H, *Hin*dIII; RI, *Eco*RI; S, *Sal*I; X, *Xba*I.

In situ hybridization on fly brains

Third instar larval brains were dissected and fixed in 10% formaldehyde in PBT. Brains were washed in PBT. In situ hybridization was performed as described by Tautz and Pfeifle (1989).

RESULTS

Replacing the *Math1* coding region with *lacZ*

The targeting construct, containing a *lacZ* cassette and a PGK-neo cassette (Fig. 1A), was used to replace the *Math1* coding region (see Materials and Methods). The targeting construct was electroporated into embryonic stem (ES) cells; 14/76 (18%) clones exhibited correct homologous recombination at the *Math1* locus (Fig. 1B).

Three ES cell lines carrying the *Math1*$^{+/\beta\text{-}gal}$ allele were injected into host blastocysts to generate chimeric mice. *Math1*$^{+/\beta\text{-}gal}$ mice were identified and intercrossed to generate homozygotes (Fig. 1C). The *Math1* deletion was confirmed by Southern analysis using both flanking and internal probes (Fig. 1A).

Math1/lacZ expression mimics *Math1* expression in the developing CNS

Analysis of the developing cerebellum at E14.5 and postnatal day 0 (P0) in *Math1*$^{+/\beta\text{-}gal}$ and *Math1*$^{\beta\text{-}gal/\beta\text{-}gal}$ mice showed that the expression pattern of the *lacZ* gene faithfully reproduced the *Math1* expression pattern observed by RNA in situ hybridization analysis (Akazawa et al., 1995; Ben-Arie et al., 1996) (Fig. 2A,B,E,G). Moreover, the cerebellar phenotype in *Math1*$^{\beta\text{-}gal/\beta\text{-}gal}$ mice (Fig. 2F,H) was identical to that observed in *Math1* null mice (Ben-Arie et al., 1997). At E14.5, the precursors of the EGL are present in the rhombic lip from which they migrate over the cerebellar anlage to populate the EGL (Fig. 2E). Mutant mice displayed far fewer of these cells than heterozygous mice (Fig. 2F). At P0, the neurons of the external granule layer (EGL) were completely lacking (Fig. 2H).

Math1/*lacZ* expression in the developing hind brain and spinal cord similarly reproduced the expression pattern of *Math1* (Fig. 2C,D). The only notable difference between the expression patterns established by in situ hybridization and X-gal staining is that β-galactosidase expression persists in differentiating or migrating cells of the spinal cord because of the stability of the β-GAL protein (Fig. 2D). In summary, the neural tissue expression pattern and cerebellar phenotype associated with the replacement of the *Math1* coding region by *lacZ* is consistent with previously published data on *Math1* expression (Akazawa et al., 1995; Ben-Arie et al., 1997, 1996; Helms and Johnson, 1998), demonstrating that the endogenous control elements were not disrupted by insertion of the *lacZ* gene. Moreover, many previously undetected clusters of *lacZ*-expressing cells became apparent upon X-gal staining of whole embryos and sections in *Math1*$^{+/\beta\text{-}gal}$ mice (see below). It is likely that limitations in the spatial resolution of RNA in situ hybridization techniques used to detect the transcript in earlier studies prevented these sites of expression from being discerned (Akazawa et al., 1995; Ben-Arie et al., 1996). Alternatively, the stability of the *lacZ* gene product and the increased sensitivity due to signal amplification allowed us to identify sites of relatively low expression levels.

Math1/*lacZ* is expressed in inner ear sensory epithelia and brain stem nuclei

The sensory organs of the inner ear were among the newly identified sites of *Math1/lacZ* expression. Expression in the otic vesicle was first detected at E12.5 and continued until E18.5 throughout much of the sensory epithelia (Bermingham et al., 1999) (Fig. 3A,B). Null mutants displayed *Math1/lacZ* expression in the inner ear throughout embryogenesis (Fig. 3C). *Math1* null mutants lack hair cells in all of the sensory organs (Bermingham et al., 1999), but maintain supporting cells, the other sensory epithelia-derived cells (Fig. 3C). These supporting cells seem to be functional, based on their morphology and the presence of overlying membranes secreted in part by these cells. Although the expression of *Math1* in inner ear sensory epithelia was not demonstrated by RNA in situ hybridization analysis, the complete lack of inner ear hair

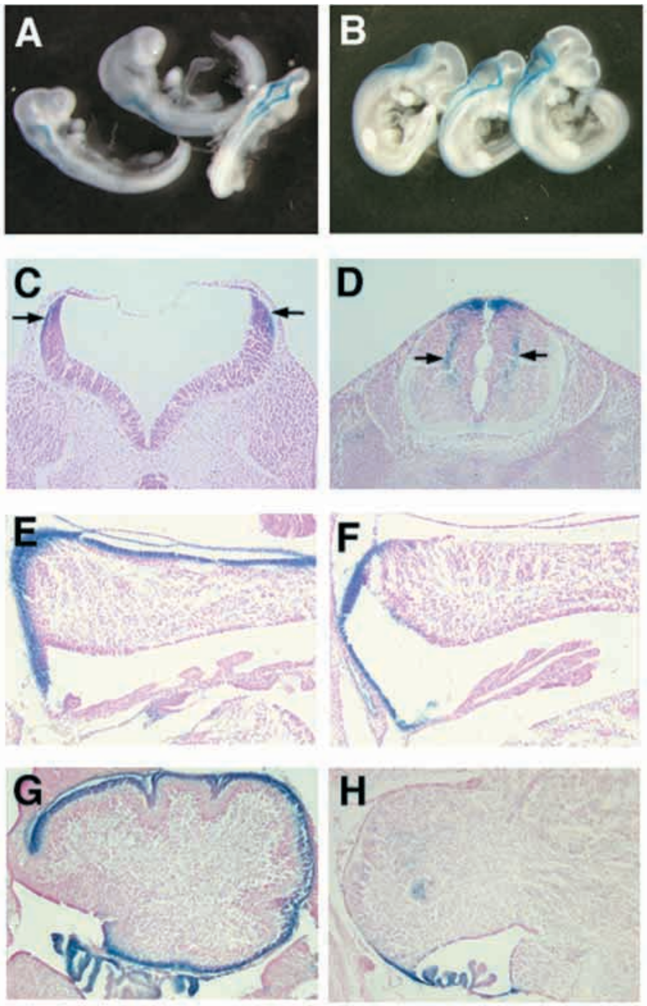

Fig. 2. *Math1/lacZ* expression and cerebellar phenotype in *Math1*$^{+/\beta\text{-}gal}$ and *Math1*$^{\beta\text{-}gal/\beta\text{-}gal}$ mice. (A) *Math1/lacZ* expression in the dorsal neural tube at E9.5 and (B) E10.5. (C) Section through the hind brain at E10.5 shows *Math1/lacZ* expression in the dorsal portion (arrows). (D) Section of the spinal cord from an E12.5 embryo, showing that dorsal cells migrate ventrally (arrows). (E) At E14.5, expression is observed in the EGL progenitors at the rhombic lip and in migrating cells that will populate the EGL. (F) In *Math1*$^{\beta\text{-}gal/\beta\text{-}gal}$ mice, *Math1/lacZ* expression is limited to a few cells in the rhombic lip, which is significantly reduced in size. (G) At P0 *Math1/lacZ* is expressed in the EGL. (H) The EGL is absent in the null mice. Original magnification for C-H, ×100.

cells in the null mutants leaves little doubt about the authenticity of the *Math1/lacZ* expression pattern.

In the brainstem *Math1/lacZ* expression appeared from E18.5 to P7 in the pons in the regions corresponding to the pontine nuclei (Fig. 3D and inset). This finding is consistent with the hypothesis of Akazawa and colleagues that *Math1*-positive cells in the developing hind brain are precursors to the bulbopontine neurons (Akazawa et al., 1995). No staining in these regions appeared in the null mutants (Fig. 3E and inset). These data raise the possibility that the absence of X-gal staining may be due to failure of precursor neurons to migrate, proliferate, and/or differentiate. Haematoxylin and eosin staining of brain stem sections from wild-type and null animals showed that null mice lack the pontine nuclei (Fig. 3F,G).

Math1/lacZ is expressed in chondrocytes

Expression of *Math1/lacZ* was detected in the developing proximal joints, such as those of the hip and shoulder, as early as E12.5 (Fig. 4A). X-gal-positive staining was detected at subsequent developmental stages in a progressive proximal-distal pattern that paralleled the normal development of joints (Fig. 4B). In the joints, *Math1/lacZ* expression immediately follows mesenchymal condensation, which begins at E11.5. Condensed mesenchyme cells differentiate into chondrocytes (Bi et al., 1999; Horton et al., 1993; Karsenty, 1998).

Chondrocytes differentiate into three subtypes during bone formation: resting, proliferating and hypertrophic. The resting chondrocytes that populate the articular cartilage are referred to as articular chondrocytes (Buckwalter and Mankin, 1998; Poole, 1997). Prior to birth, resting chondrocytes constitute the entire chondrocyte population in joints. To establish which cells expressed *Math1/lacZ*, sections from E18.5 and P7 *Math1*$^{+/\beta\text{-}gal}$ mice were stained with X-gal. *Math1/lacZ* is expressed in the resting chondrocytes of all joints analyzed at E18.5; resting chondrocytes in the elbow joint are shown in Fig. 4C, and Fig. 4D shows the resting, proliferating and articular chondrocytes of a P7 mouse. We also examined joints of E18.5 embryos with anti-MATH1 antibody and found expression in resting chondrocytes, whereas no expression was observed in null embryos (data not shown). It should be noted that not all articular cartilage cells express *Math1/lacZ* (Fig. 4E). *Math1/lacZ* expression in *Math1* null mutants is similar to that in heterozygous mice at E18.5, suggesting that *Math1* is not required for resting chondrocyte development. Since *Math1* null mice die at birth, however, we cannot asses the role of *Math1* in the development of proliferating and articular chondrocytes or ossification.

Math1/lacZ is expressed in Merkel cells

By E14.5 *Math1/lacZ*-positive cells were apparent around the vibrissae and in the skin of much of the body (Fig. 4B). In the trunk, the stained cells were arranged in a striped pattern defined by the epidermal ridges. This staining was apparent only in the hairy, not the glabrous, skin. All the primary (mystical) vibrissae, including the lateral nasal, maxillary and four large hairs, were positive for *Math1/lacZ*. Staining was also detected in the secondary vibrissae, including the labial, submental, rhinal and isolated orbital vibrissae (supra-, infra- and post-orbital) (Yamakado and Yohro, 1979). By E15.5 staining appeared in clusters of cells in the foot pads (Fig. 4B).

To identify the *Math1/lacZ*-positive cells in the vibrissae, footpad and hairy skin, we examined histological sections from *Math1*$^{+/\beta\text{-}gal}$ mice (Fig. 5A-D). Sections through the vibrissae showed that the stained cells are localized to the more apical half of the hair shaft, but are not in the hair itself. Cross sections through the foot pad illustrated staining of clusters of cells in the epidermal layer (Fig. 5B,C). As shown in Fig. 5D, sections through the truncal skin identified clusters of *Math1/lacZ*-stained cells. The stained cells were arranged in a horseshoe-shaped pattern centered within an elevated button-like structure in the hairy skin. These button-like structures were identified as touch domes or *Haarscheiben* (Pinkus, 1905), which are characterized by a thickened epidermis and an elevated dermal papilla with a capillary network. Touch domes are associated with large guard hairs dispersed between other hair types in the

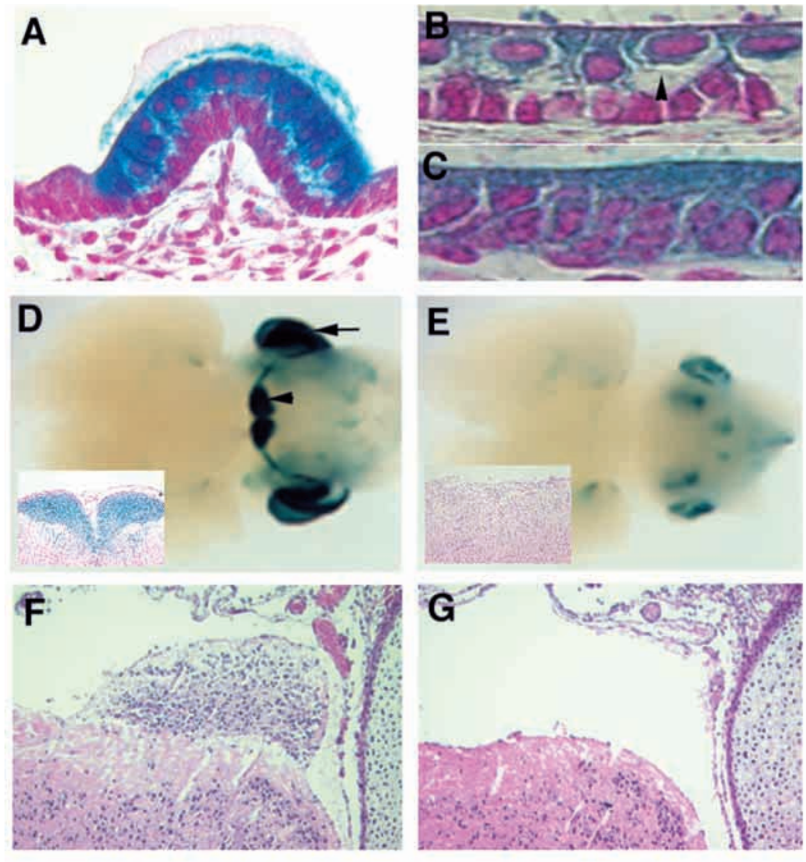

Fig. 3. Expression of *Math1/lacZ* in the inner ear and brain stem and histological analysis of the pontine nuclei. X-gal staining of E18.5 *Math1*$^{+/\beta\text{-}gal}$ utricular crista (A) and inner ear sensory epithelia of (B) *Math1*$^{+/\beta\text{-}gal}$ and (C) *Math1*$^{\beta\text{-}gal/\beta\text{-}gal}$. Note *Math1/lacZ* expression in the upper hair cell layer of the sensory epithelia in A and B, and the characteristic calyx appearance (arrowhead). In the null mice X-gal staining of epithelial cells is non-specific in the absence of hair cells (C). Whole-brain X-gal staining of *Math1*$^{+/\beta\text{-}gal}$ (D) and *Math1*$^{\beta\text{-}gal/\beta\text{-}gal}$ (E) at E18.5. Note the positive staining of the pontine nuclei (arrowhead) and cerebellum (arrow) in *Math1*$^{+/\beta\text{-}gal}$ mice, both of which are lacking or greatly reduced in null mutants (inset). (F and G) Haematoxylin and eosin staining of sagittal sections through the pons of a wild-type (F) and null mutant (G) show the loss of pontine nuclei in null mutants. Original magnifications: (A) ×400; (B,C) ×1000; (D,E) ×8; inset in (D,E) ×100; (F,G) ×10.

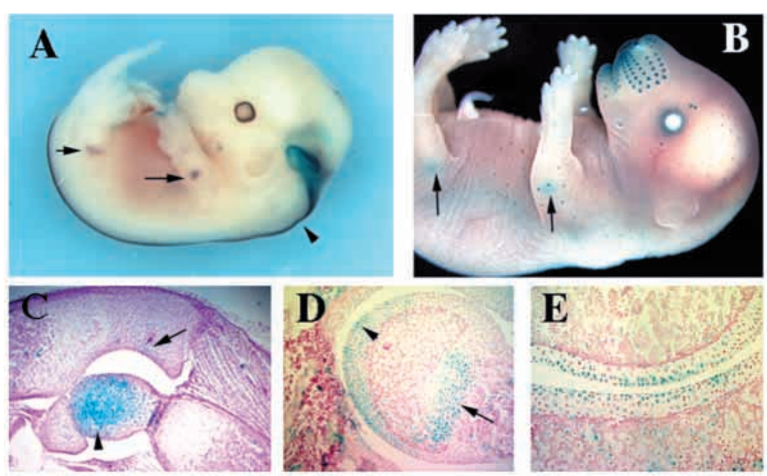

Fig. 4. *Math1/lacZ* is expressed in joint chondrocytes. X-gal staining of whole embryos at (A) E12.5 and (B) E16.5 illustrates that *Math1/lacZ* is expressed in all joints. (C) Horizontal section through the elbow joint of E18.5 *Math1*$^{+/\beta\text{-}gal}$ mouse shows that it is expressed in resting chondrocytes (arrow). (D) A horizontal section through a humero-radial joint at P10 shows that it is expressed in the articular chondrocytes (arrowhead) and resting chondrocytes (arrow). (E) High magnification of a section through a wrist joint showing *Math1/lacZ* is expressed in articular chondrocytes. Original magnification (C) ×10; (D) ×20; (E) ×40.

coat. The spatial distribution of *Math1/lacZ*-stained cells, the timing of their appearance at E14.5, and their localization within the mystical pads of the vibrissae and the touch domes in the hairy skin suggest that these cells correspond to Merkel cells, specialized cells in the epidermis that form slow-adapting type I mechanoreceptor complexes with neurites (see below and Munger, 1991).

The results of comparative analysis of the *Math1/lacZ* expression pattern in heterozygous and homozygous E16.5 animals are shown in Fig. 5E-L. *Math1*$^{\beta\text{-}gal/\beta\text{-}gal}$ embryos displayed a staining pattern similar to that of *Math1*$^{+/\beta\text{-}gal}$ littermates in the vibrissae and footpads (Fig. 5E and I, G and K), although the staining was more intense because of the *lacZ* dosage effect. In contrast, staining in the touch domes of the hairy skin was barely detectable in *Math1*$^{\beta\text{-}gal/\beta\text{-}gal}$ embryos (Fig. 5F and J, H and L). The reduction of staining in null animals was also obvious at E18.5 (not shown).

To further define *Math1/lacZ*-positive cells in the skin, *Math1*$^{+/\beta\text{-}gal}$ mice were mated to *Tabby* mice. *Tabby* (*Ta*) is a spontaneous X-linked mutation displaying a similar phenotype in hemizygous males and homozygous females (Ferguson et al., 1997). *Tabby* mutants lack guard hair follicles (tylotrich), a subset of follicles that are associated with touch domes in the hairy skin of the trunk (Vielkind et al., 1995), and some of the

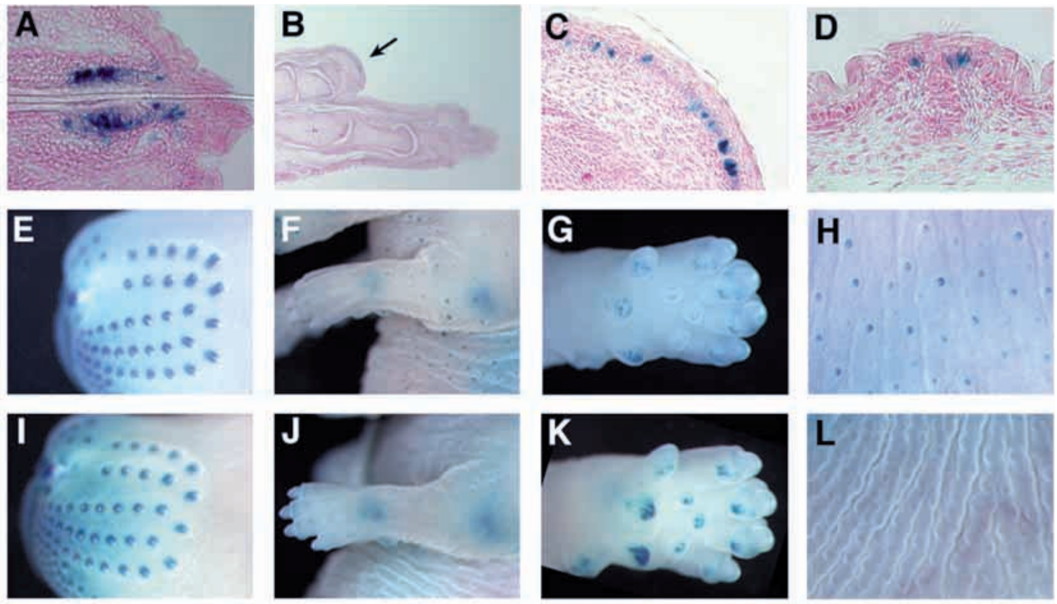

Fig. 5. *Math1/lacZ* expression in Merkel cells. To identify the structures stained on the hairy and non-hairy skin, E16.5 littermate embryos were stained as whole mounts, sectioned, and microscopically examined. Shown are sections through the vibrissae (A), foot pad at low (B) and high (C) magnification of the region marked by an arrow in B, and (D) hairy skin. In all sections the localization of the stained cells was as expected from Merkel cells. Close-up pictures were taken through a stereomicroscope of *Math1*$^{+/\beta\text{-}gal}$ (control, panels E-H) and *Math1*$^{\beta\text{-}gal/\beta\text{-}gal}$ (null, I-L) littermate mice. Staining in null mice appeared stronger because of a dosage effect in the vibrissae (E,I), limb joints (F,J) and foot pads (G,K). In contrast, the staining intensity of null (J,L) mice was markedly weaker than that of heterozygous (F,H) mice in the touch domes associated with the hairy skin. Original magnification: (A) ×200; (B) ×50; (C) ×400; (D) ×500; (E,G-I,K,L) ×32; F,J ×16.

five secondary vibrissae on the head (Gruneberg, 1971). Hence, in a cross of *Ta*/*Ta* females with a heterozygous *Math1*$^{+/\beta\text{-}gal}$ male, 50% of the male progeny are *Ta*/Y: *Math1*$^{+/\beta\text{-}gal}$, allowing us to assess whether the *Math1/lacZ*-positive cells correspond to Merkel cells.

Both *Tabby* females and males carrying the *Math1*$^{+/\beta\text{-}gal}$ allele displayed X-gal staining in the vibrissae and foot pads (Fig. 6A,B and data not shown). The effect of the *Tabby* mutation on the number of secondary vibrissae was quite clear: hemizygous males completely lacked *Math1/lacZ*-positive cells around the missing secondary vibrissae (typically lacking in *Ta* mutants) and on the trunk (Fig. 6E). Females that are heterozygous for *Tabby* showed patchy staining in the touch domes (although less than wt), as should be anticipated in female carriers of a mutation in a gene that undergoes random X chromosome inactivation (Fig. 6C,D). The localization and distribution of the positive cells, as well as their absence in selected vibrissae and the trunk of *Tabby* males, strongly indicate that *Math1* is expressed in the Merkel cells associated with guard follicles in the touch domes of the hairy skin.

To ascertain whether the *Math1/lacZ* expression pattern reflects the normal *Math1* expression pattern, immunohistochemical analysis of MATH1 was performed on sections from abdominal skin. As seen in Fig. 7A and B, MATH1-positive cells were detected around the hair follicles of *Math1*$^{+/+}$ but not *Math1*$^{\beta\text{-}gal/\beta\text{-}gal}$ mice. Antibodies against two Merkel cells markers were chosen for further analysis: anti-cytokeratin18, expressed in simple epithelia, and chromogranin, localized to secretory granules of neuroendocrine, endocrine, and neuronal tissues. Both cytokeratin 18 (Fig. 7C,D) and chromogranin A (Fig. 7E,F) confirmed the identity of the *Math1/lacZ*-positive cells as Merkel cells, but did not reveal staining abnormalities in *Math1*$^{\beta\text{-}gal/\beta\text{-}gal}$ mice. Thus, *Math1* does not seem to be essential for the genesis of the neuroendocrine Merkel cells. Because *Math1* null mutants die at birth, we cannot assess the functional integrity of Merkel cells in these mutants.

Math1 partially rescues CHOs in flies deleted for *ato*

Given the remarkable similarity in expression patterns of *ato*

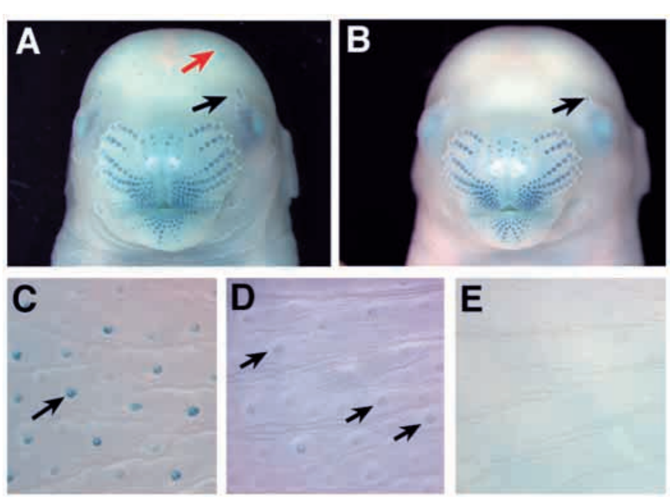

Fig. 6. Lack of X-gal-stained touch domes in *Tabby* mice. *Tabby/Tabby* females were crossed with *Math1*$^{+/\beta\text{-}gal}$ males, and their progeny were X-gal stained and gender-determined at E16.5. Staining around primary vibrissae in the snout was detected in both female embryos heterozygous for the *Tabby* mutation (A) and male embryos hemizygous for the mutation (B). Secondary vibrissae, which are known to vary in number in the *Tabby* mutants (black arrows), were also stained. The staining of the touch domes was less intense in the *Tabby*/X female (D) than *Math1*$^{+/\beta\text{-}gal}$ (wt for *Tabby*) embryos (C), since *Tabby* is a semidominant mutation. However, patches of stained touch domes were detected in a female embryo that carried a wild-type allele at the *Tabby* locus (A, red arrow, and D). In contrast, a hemizygous male (B,E) completely lacked staining and touch domes, due to the loss of hair follicles that abolishes the development of Merkel cells.

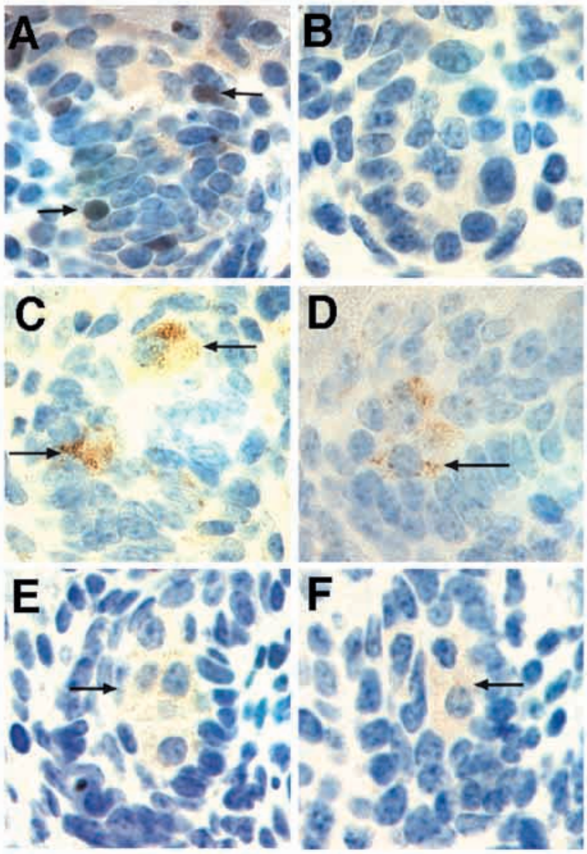

Fig. 7. Marker analysis of Merkel cells in wild-type and *Math1* null mice. Skin sections from *Math1*$^{+/+}$ and *Math1*$^{\beta\text{-}gal/\beta\text{-}gal}$ reacted with antibodies against *Math1* (A,B), cytokeratin 18 (C,D), and chromogranin A (E,F). Polyclonal antibodies to MATH1 identify multiple basal nuclei (arrows) in rare abdominal hair follicles of wild-type (A) but not mutant mice (B). Monoclonal antibodies to cytokeratin 18 and chromogranin A identify Merkel cells (arrows) in both wild-type (C,E) and mutant (D,F) mice. Original magnification ×100.

and *Math1*, and their identical basic domains, we wondered if *Math1* would mimic the effects of *ato* overexpression by producing ectopic chordotonal organs. Expressing *Math1* during pupal development by heat shock using the UAS-Gal4 system (Brand and Perrimon, 1993) resulted in supernumerary external sense organs on the notum (Fig. 8A,B) and the wing blade (data not shown), as reported for *ato* (Jarman et al., 1993) and the Achaete-Scute complex (AS-C) genes (Rodriguez et al., 1990). *Math1* expression, like *ato*, produced ectopic chordotonal organs (Fig. 8G), although with less efficiency than *ato* (A. Jarman, personal communication). Overexpression of the AS-C genes does not, however, result in ectopic chordotonal organs (Jarman et al., 1993). *Math1* thus has a similar functional specificity to *ato*.

Since several *ato* enhancers are *ato*-dependent (Sun et al., 1998), they may be activated by *Math1*, which would then lead to ectopic CHO specification. To determine whether *Math1* can substitute for *ato* function in the fly, and to rule out the possibility that production of CHOs by *Math1* is due to *ato* activation, we expressed *Math1* in *ato* mutant embryos. The mutants lack all chordotonal neurons (Fig. 8D), but overexpressing *Math1* partially rescues the loss of these neurons (Fig. 8E) in a manner similar to *ato* (Chien et al., 1996).

DISCUSSION

Over the past few years significant progress has been made towards unraveling the roles of bHLH proteins in vertebrate neurogenesis. Neural vertebrate bHLH-encoding genes were isolated and characterized because *Drosophila* homologues such as *ato* or the AS-C genes had been previously shown to be required for neurogenesis (Anderson, 1995; Guillemot,

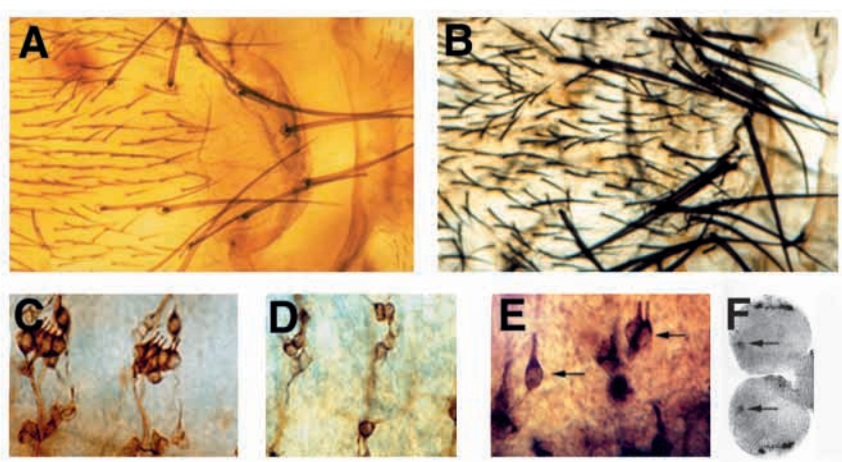

G	Wing Hinge	Third Wing Vein	Scutellum
Wild Type	++	-	-
hs-Gal4/UAS-Math1	+++	+	+

Fig. 8. *Math1* rescues the lack of chordotonal neurons in *Drosophila ato* mutant embryos. (A) Dorsal view of the thorax of a wild-type fly. Note regular array of bristles or macrochaetae. (B) Similar view of a transgenic fly in which *Math1* was overexpressed using the UAS/GAL4 system (Brand and Perrimon, 1993). This ectopic expression leads to numerous extra bristles that are external sensory organs, not CHOs. Ectopic CHOs were produced in many other regions (data not shown). (C) Lateral view of two abdominal clusters containing 6 CHOs in addition to external sensory organs, revealed by a neuronal-specific antibody (mAb 22C10). The 5 lateral CHOs form a cluster, and the sixth is dorsal to the cluster. (D) Similar view of an *ato* mutant embryo showing lack of the CHOs. (E) Ubiquitous expression of *Math1* induces new CHO neurons (arrows) in *ato* mutant embryos in the proper location. (F) In situ hybridization of whole mount third instar brain using the *ato* cDNA as a probe. Note expression in the developing optic lobes (‘horse shoe’ expression patterns) and two punctate clusters of cells in the middle of the brain lobes (arrows). (G) *Math1* expression in *Drosophila* induces CHO formation in normal and ectopic locations. (+) indicates presence of CHOs and (–) indicates their absence. Number of (+) in the first column is used to quantify the relative increase in the number of CHOs observed when *Math1* is expressed.

1995; Lee, 1997; Takebayashi et al., 1997). Indeed, several genes were shown to be proneural because their absence caused a failure of neuroblast or sensory organ precursor (SOP) specification, whereas their overexpression lead to the recruitment of supernumerary neuronal precursors (Ghysen and Dambly-Chaudiere, 1989). With the exception of neurogenin (Ngn) 1 and 2 (Fode et al., 1998; Ma et al., 1998), it remains uncertain which of the vertebrate homologues play roles similar to their *Drosophila* counterparts, and what precise role different bHLH proteins play in neural development. In *Drosophila*, *ato* is required for the development of a specific subset of sense organs, the chordotonal organs (Jarman et al., 1993). CHOs are internal mechanosensors of the PNS (McIver, 1985). Thus, *ato* and the CHOs provide an excellent system in which to ascertain not only the molecular and developmental relationship between invertebrate and vertebrate neurogenesis vis-à-vis the function of the proneural genes, but also the evolutionary conservation of sensory organ function and specification.

Seven *ato* homologues have been cloned and analyzed in the mouse: Mouse Atonal Homologues (MATH) 1, 2, 3, 4A (also known as Ngn2), 4B (Ngn3), 4C (Ngn1), and 5 (Akazawa et al., 1995; Bartholomä and Nave, 1994; Ben-Arie et al., 1997, 1996; Fode et al., 1998; Ma et al., 1998; McCormick et al., 1996; Shimizu et al., 1995; Takebayashi et al., 1997). Most are expressed during neurogenesis in both the CNS and PNS. These homologues vary in the degree of their sequence conservation, and may be divided into three groups. The most distantly related group, the neurogenins, includes Ngn 1, 2 and 3. These gene products share, on average, 53% identity in the bHLH domain with ATO. They are expressed largely in mitotic CNS and sensory ganglia progenitor cells. Recent work suggests that these genes may play a role in neuroblast determination, and may therefore be true proneural genes (Fode et al., 1998; Ma et al., 1998). The second group includes MATH2 and MATH3, which share 57% identity in the bHLH domain with ATO. These proteins have been postulated to function in postmitotic neural cells (Bartholomä and Nave, 1994; Shimizu et al., 1995). *Math2* expression is confined to the CNS, while *Math3* is expressed in both the CNS and the trigeminal and dorsal root ganglia. The third group includes MATH1 and MATH5, arguably the only true *ato* homologues by amino acid sequence criteria, sharing 67% and 71% identity with the bHLH domain of ATO, respectively. It is noteworthy that both genes encode a basic domain identical to that of ATO. Interestingly, the basic domain of ATO was shown to be sufficient, in the context of another proneural protein (SCUTE), to substitute for the loss of *ato* function (Chien et al., 1996). *Math1* was initially shown to be expressed in the precursors of the cerebellar EGL and in the dorsal spinal cord (Ben-Arie et al., 1997, 1996). *Math5* is expressed in the dividing progenitors in the developing retina and in the vagal ganglion (Brown et al., 1998).

With the exception of *Math5* expression in the neural retina, these observations pose a paradox: none of the vertebrate homologs appeared to be expressed in peripheral organs or tissues similar to those where *ato* is expressed. Jarman et al. (1993) reported that *ato* is expressed in the CNS. In this study we show that, in addition to the inner proliferation center of the optic lobe, *ato* is expressed in a small anteriomedial patch of cells in each brain lobe (Fig. 8F). Because it remains unclear, however, precisely what role *ato* plays in *Drosophila* CNS development, it has been difficult to argue that *ato* and its vertebrate homologues display functional conservation.

Our experiments reveal sites of previously uncharacterized *Math1* expression. As expected, we found that *Math1/lacZ* expression in the CNS corresponds to that of *Math1*, but we also found that *Math1* is expressed in the skin, the joints, and the inner ear, in striking parallel to *ato* expression in the fly. Moreover, the expression in the ear (sensory epithelium) and the skin (Merkel cells) is restricted to sensory structures whose function is to convert mechanical stimuli into neuronal electrochemical signals. It is important to point out that in *Drosophila*, *ato* appears to play two roles simultaneously. It is required not only to select the precursors of the CHOs (proneural role), but also to specify these precursors as CHO precursors (lineage identity role) (Jarman and Ahmed, 1998; Jarman et al., 1993). The specificity of *Math1* expression in the periphery makes it tempting to speculate that it, too, may endow specific cells with very specific lineage identities to distinguish them functionally from other sensory structures. The ability of *Math1* to induce ectopic CHO formation and to restore CHOs to *ato* mutant embryos supports the notion that *Math1*, and particularly its basic domain, encodes lineage identity information not unlike that encoded by *ato*. This suggests that the mammalian cells expressing *Math1*, at least in the ear and the skin, are functionally similar and perhaps evolutionarily related to *Drosophila* cells that require *ato*. Furthermore, *Math5* expression in the neural retina suggests that the functions of *atonal* in the fly are carried out by two genes in the mouse: the development of some mechanoreceptors is under the control of *Math1* and retinal development is possibly under the control of *Math5*. It is interesting to note that in the fully sequenced nematode *C. elegans*, only one homolog of *atonal*, *lin-32*, was identified (Zhao and Emmons, 1995). Mutants with the *u282* allele are touch-insensitive, which strengthens the argument for evolutionary conservation of atonal function in mechanoreception.

The pattern of *Math1/lacZ* expression in the pontine nuclei led us to carefully evaluate this region in null mutants. Although we did not previously detect defects in the pons of *Math1* null mice (Ben-Arie et al., 1997), closer analysis revealed the lack of pontine nuclei at this site. These neurons derive from the rhombic lip (Altman and Bayer, 1996) as do the EGL neurons, which are also lacking in *Math1* null mice.

While it is possible to draw parallels between *Math1* and *ato* expression in the skin and ear, it is not clear that such is the case for the joints. *ato* expression in the fly joints is required for the formation of leg CHOs. In contrast, *Math1* is expressed in resting and articular chondrocytes that do not have any described neural function, and for which no parallels exist in the fly. It may be that *Math1* expression in cartilage indicates a novel role for a mechanosensory gene, or it may simply reflect similarities in the molecular events underlying the development of the various *Math1*-expressing cell types. Alternatively, CHOs may also function as joint structural elements in the fly, or articular cartilage may have a mechanoreceptive or transducive capacity yet to be described. There is no evidence at this point to support one or another of these possibilities. We must await the generation of mice with a joint-specific *Math1* mutation.

It will be interesting to determine whether *Math1* and *ato* have similar roles and regulate similar molecular pathways. For example, is *Math1* a proneural gene in at least some of the tissues in which it is expressed? Does it play a determining role in some tissues, but a differentiating role in others? Does *Math1*, like *ato*, function in a Notch-Delta-dependent pathway? Does it activate the epidermal growth factor receptor pathway in neighboring cells? Analyzing the functions of *ato* and *Math1* will enhance our understanding of neural development and the evolutionary conservation of sensory function. The sites and specificity of *Math1* expression may make it suitable as a tool of gene therapy or gene activation approaches to illnesses such as hearing loss and osteoarthritis that are due to age-related or environmental damage.

The authors gratefully acknowledge the expert assistance of Barbara Antalffy in the Neuropathololgy Core of the Mental Retardation Research Center at Baylor College of Medicine. We thank P. Overbeek for Tabby mice, and A. Grossler for the selection cassette. B. A. H. is funded by an NIH postdoctoral fellowship. Portions of this work were supported by a grant from NASA. H. J. B. and H. Y. Z. are investigators of the Howard Hughes Medical Institute.

REFERENCES

Akazawa, C., Ishibashi, M., Shimizu, C., Nakanishi, S. and Kageyama, R. (1995). A mammalian helix-loop-helix factor structurally related to the product of *Drosophila* proneural gene *atonal* is a positive transcriptional regulator expressed in the developing nervous system. *J. Biol. Chem.* **270**, 8730-8738.

Alder, J., Cho, N. and Hatten, M. (1996). Embryonic precursor cells from the rhombic lip are specified to a cerebellar granule neuron identity. *Neuron* **17**, 389-399.

Altman, J. and Bayer, S. A. (1996). *Development of the Cerebellar System: in Relation to its Evolution, Sturcture, and Functions*. Boca Raton, Florida: CRC Press.

Anderson, D. J. (1995). Neural development. Spinning skin into neurons. *Curr. Biol.* **5**, 1235-1238.

Bartholomä, A. and Nave, K. A. (1994). NEX-1: a novel brain-specific helix-loop-helix protein with autoregulation and sustained expression in mature cortical neurons. *Mech. Dev.* **48**, 217-228.

Ben-Arie, N., Bellen, H. J., Armstrong, D. L., McCall, A. E., Gordadze, P. R., Guo, Q., Matzuk, M. M. and Zoghbi, H. Y. (1997). *Math1* is essential for genesis of cerebellar granule neurons. *Nature* **390**, 169-172.

Ben-Arie, N., McCall, A. E., Berkman, S., Eichele, G., Bellen, H. J. and Zoghbi, H. Y. (1996). Evolutionary conservation of sequence and expression of the bHLH protein Atonal suggests a conserved role in neurogenesis. *Hum. Mol. Gen.* **5**, 1207-1216.

Bermingham, N. A., Hassan, B. A., Price, S. D., Vollrath, M. A., Ben-Arie, N., Eatock, R. A., Bellen, H. J., Lysakowski, A. and Zoghbi, H. Y. (1999). *Math1*: An essential gene for the generation of inner ear hair cells. *Science* **284**, 1837-1841.

Bi, W., Deng, J. M., Zhang, Z., Behringer, R. R. and de Crombrugghe, B. (1999). *Sox9* is required for cartilage formation. *Nat. Genet.* **22**, 85-89.

Bonnerot, C. and Nicolas, J. F. (1993). Application of LacZ gene fusions to postimplantation development. *Methods Enzymol.* **225**, 451-469.

Boyan, G. S. (1993). Another look at insect audition: the tympanic receptors as an evolutionary specialization of the chordotonal system. *J. Insect Physiol.* **39**, 187-200.

Brand, A. H. and Perrimon, N. (1993). Targeted gene expression as a means of altering cell fates and generating dominant phenotypes. *Development* **118**, 401-415.

Brown, N. L., Kanekar, S., Vetter, M. L., Tucker, P. K., Gemza, D. L. and Glaser, T. (1998). *Math5* encodes a murine basic helix-loop-helix transcription factor expressed during early stages of retinal neurogenesis. *Development* **125**, 4821-4833.

Buckwalter, J. A. and Mankin, H. J. (1998). Articular cartilage: tissue design and chondrocyte-matrix interactions. *Instr. Course Lect.* **47**, 477-86.

Chien, C. T., Hsiao, C. D., Jan, L. Y. and Jan, Y. N. (1996). Neuronal type information encoded in the basic-helix-loop-helix domain of proneural genes. *Proc. Natl. Acad. Sci. USA* **93**, 13239-13244.

Davis, R. L., Cheng, P. F., Lassar, A. B. and Weintraub, H. (1990). The *MyoD* DNA binding domain contains a recognition code for muscle-specific gene activation. *Cell* **60**, 733-746.

Dreller, C. and Kirschner, W. H. (1993). Hearing in honeybees: localization of the audiotory sense organ. *J. Comp. Physiol. A* **173**, 275-279.

Eberl, D. F. (1999). Feeling the vibes: chordotonal mechanisms in insect hearing. *Curr. Opin. Neurobiol.* **9**, 389-393.

Ferguson, B. M., Brockdorff, N., Formstone, E., Ngyuen, T., Kronmiller, J. E. and Zonana, J. (1997). Cloning of *Tabby*, the murine homolog of the human *EDA* gene: evidence for a membrane-associated protein with a short collagenous domain. *Hum. Mol. Genet.* **6**, 1589-1594.

Fode, C., Gradwohl, G., Morin, X., Dierich, A., LeMeur, M., Goridis, C. and Guillemot, F. (1998). The bHLH protein NEUROGENIN 2 is a determination factor for epibranchial placode-derived sensory neurons. *Neuron* **20**, 483-494.

Friedrich, G. and Soriano, P. (1991). Promoter traps in embryonic stem cells: a genetic screen to identify and mutate developmental genes in mice. *Genes Dev.* **5**, 1513-1523.

Ghysen, A. and Dambly-Chaudiere, C. (1989). Genesis of the *Drosophila* peripheral nervous system. *Trends Genet.* **5**, 251-255.

Gruneberg, H. (1971). The tabby syndrome in the mouse. *Proc. R. Soc. Lond. B (Biol. Sci.)* **179**, 139-156.

Guillemot, F. (1995). Analysis of the role of basic-helix-loop-helix transcription factors in the development of neural lineages in the mouse. *Biol. Cell* **84**, 227-241.

Hatten, M. E. and Heintz, N. (1995). Mechanisms of neural patterning and specification in the developing cerebellum. *Ann. Rev. Neurosci.* **18**, 385-408.

Helms, A. W. and Johnson, J. E. (1998). Progenitors of dorsal commissural interneurons are defined by MATH1 expression. *Development* **125**, 919-928.

Horton, W. A., Machado, M. A., Ellard, J., Campbell, D., Putnam, E. A., Aulthouse, A. L., Sun, X. and Sandell, L. J. (1993). An experimental model of human chondrocyte differentiation. *Prog. Clin. Biol. Res.* **383B**, 533-540.

Jarman, A. P. and Ahmed, I. (1998). The specificity of proneural genes in determining *Drosophila* sense organ identity. *Mech. Dev.* **76**, 117-125.

Jarman, A. P., Grau, Y., Jan, L. Y. and Jan, Y. N. (1993). *atonal* is a proneural gene that directs chordotonal organ formation in the *Drosophila* peripheral nervous system. *Cell* **73**, 1307-1321.

Kania, A., Salzberg, A., Bhat, M., D'Evelyn, D., He, Y., Kiss, I. and Bellen, H. J. (1995). *P*-element mutations affecting embryonic peripheral nervous system development in *Drosophila melanogaster*. *Genetics* **139**, 1663-1678.

Karsenty, G. (1998). Genetics of skeletogenesis. *Dev. Genet.* **22**, 301-313.

Lee, J. E. (1997). Basic helix-loop-helix genes in neural development. *Curr. Opin. Neurobiol* **7**, 13-20.

Lee, K. J., Mendelsohn, M. and Jessell, T. M. (1998). Neuronal patterning by BMPs: a requirement for GDF7 in the generation of a discrete class of commissural interneurons in the mouse spinal cord. *Genes Dev.* **12**, 3394-3407.

Liu, X. Y., Dangel, A. W., Kelley, R. I., Zhao, W., Denny, P., Botcherby, M., Cattanach, B., Peters, J., Hunsicker, P. R., Mallon, A. M., Strivens, M. A., Bate, R., Miller, W., Rhodes, M., Brown, S. D. and Herman, G. E. (1999). The gene mutated in bare patches and striated mice encodes a novel 3beta-hydroxysteroid dehydrogenase. *Nat. Genet.* **22**, 182-187.

Ma, Q., Chen, Z., del Barco Barrantes, I., de la Pompa, J. L. and Anderson, D. J. (1998). *neurogenin1* is essential for the determination of neuronal precursors for proximal cranial sensory ganglia. *Neuron* **20**, 469-482.

McCormick, M. B., Tamimi, R. M., Snider, L., Asakura, A., Bergstrom, D. and Tapscott, S. J. (1996). *NeuroD2* and *neuroD3*: distinct expression patterns and transcriptional activation potentials within the *neuroD* gene family. *Mol. Cell. Biol.* **16**, 5792-800.

McIver, S. B. (1985). Mechanoreception. In *Comprehensive Insect Physiology, Biochemistry, and Pharmacology* (ed. G. A. Kerkut and L. I. Gilbert), pp. 71-132. Oxford: Pergamon Press.

Moulins, M. (1976). Ultrastructure of chordotonal organs. In *Structure and Function of Proprioceptors in the Invertebrates* (ed. P. J. Mill), pp. 387-426. London: Chapman and Hall.

Munger, B. L. (1991). The Biology of Merkel Cells. In *Physiology, Biochemistry, and Molecular Biology of the Skin.* Second edition (ed. L. A. Goldsmith), pp. 836-856. Oxford, UK: Oxford University Press.

Pinkus, F. (1905). Über Hautsinnesorgane neben dem menschlichen Haar

(Haarscheiben) und ihre verglei chend-anatomische Bedeutung. *Arch. Mikr. Anat.* **65**, 121-179.

Poole, C. A. (1997). Articular cartilage chondrons: form, function and failure. *J. Anat.* **191**, 1-13.

Rodriguez, I., Hernandez, R., Modolell, J. and Ruiz-Gomez, M. (1990). Competence to develop sensory organs is temporally and spatially regulated in *Drosophila* epidermal primordia. *EMBO J.* **9**, 3583-3592.

Shimizu, C., Akazawa, C., Nakanishi, S. and Kageyama, R. (1995). *MATH-2*, a mammalian helix-loop-helix factor structurally related to the product of *Drosophila* proneural gene *atonal*, is specifically expressed in the nervous system. *Eur. J. Biochem.* **229**, 239-248.

Sun, Y., Jan, L. Y. and Jan, Y. N. (1998). Transcriptional regulation of atonal during development of the *Drosophila* peripheral nervous system. *Development* **125**, 3731-3740.

Takebayashi, K., Takahashi, S., Yokota, C., Tsuda, H., Nakanishi, S., Asashima, M. and Kageyama, R. (1997). Conversion of ectoderm into a neural fate by *ATH-3*, a vertebrate basic helix-loop-helix gene homologous to *Drosophila* proneural gene *atonal*. *EMBO J.* **16**, 384-395.

Tautz, D. and Pfeifle, C. (1989). A nonradioactive *in situ* hybridization method for the localization of specific RNAs in *Drosophila* embryos reveals translation control of the segmentation gene *hunchback*. *Chromosoma* **98**, 81-85.

Vaessin, H., Caudy, M., Bier, E., Jan, L. Y. and Jan, Y. N. (1990). Role of helix-loop-helix proteins in *Drosophila* neurogenesis. *Cold Spring Harb. Symp. Quant. Biol.* **55**, 239-245.

van Staaden, M. J. and Römer, H. (1998). Evolutionary transition from stretch to hearing organs in ancient grasshoppers. *Nature* **384**, 773-776.

Vielkind, U., Sebzda, M. K., Gibson, I. R. and Hardy, M. H. (1995). Dynamics of Merkel cell patterns in developing hair follicles in the dorsal skin of mice, demonstrated by a monoclonal antibody to mouse keratin 18. *Acta Anat.* **152**, 93-109.

Yamakado, M. and Yohro, T. (1979). Subdivision of mouse vibrissae on an embryological basis, with descriptions of variations in the number and arrangement of sinus hairs and cortical barrels in BALB/c (*nu/+; nude, nu/nu*) and hairless (*hr/hr*) strains. *Am. J. Anat.* **155**, 153-173.

Zhao, C. and Emmons, S. W. (1995). A transcription factor controlling development of peripheral sense organs in *C. elegans*. *Nature* **373**, 74-78.